Ground Validation of the Inertial Stellar Compass[1,2]

T. Brady, S. Buckley, C. Tillier
Charles Stark Draper Laboratory, Inc.
555 Technology Square, MS27, Cambridge, MA 02139
phone: (617) 258-2366 email: tbrady@draper.com

Abstract—The Inertial Stellar Compass (ISC), under development at Draper Laboratory, provides spacecraft attitude determination to 0.1 degree accuracy using just 3.5 W of power. This paper describes the process of validating the performance of the instrument on the ground prior to characterizing it on orbit. Starting with subsystem-level testing of the ISC's active pixel sensor camera and MEMS (MicroElectroMechanical System) 3-axis gyro board, we describe the operations leading up to integrated system testing of the camera and gyro sensor outputs, which are combined to provide a robust attitude solution over a wide range of operating conditions. Under the guidance of NASA's New Millennium Program, the ground validation process, which will be followed by an on-orbit demonstration, will make feasible a new class of low-power, integrated attitude sensors for small spacecraft.

TABLE OF CONTENTS

1. INTRODUCTION 1
2. VALIDATION APPROACH 2
3. GROUND VALIDATION 3
4. LESSONS LEARNED 11
5. CONCLUSIONS 12
REFERENCES 12
ACKNOWLEDGEMENTS 12
BIOGRAPHIES 13

1. INTRODUCTION

The ISC is an innovative attitude determination sensor that combines MEMS and APS technologies in an integrated package to produce a real-time, robust attitude solution and rate estimate. Among the key advantages of the ISC are its low power, ease of integration with a host spacecraft, and ability to maintain better than 0.1º accuracy during high rate (up to 40º/sec) maneuvers. Key ISC performance features include:

- Better than 0.1º (1-sigma) accuracy in each axis
- High-rate maneuver capability (up to 40º/sec)
- Self-initialization (over 99% of the sky)
- Low Mass ~ 2.9 kg
- Low Power ~ 3.5 W

This paper provides an overview of the integration and test (I&T) process, rather than a quantitative discussion of performance results. By supporting ground validation, NASA's New Millennium Program's ST6 Project is providing a technology infusion path for the ISC. These efforts will reduce both cost and risk and bring new and useful technologies to future spacecraft designs.

The ISC program is nearing the conclusion of the ground validation phase. The instrument has been extensively tested and has demonstrated promising results. The intent of this paper is to share methods and experience in integrating and testing this new class of attitude determination sensor. Lessons learned are provided to support continuous improvement in spacecraft instrumentation technologies.

Technical Overview of the ISC

The ISC consists of two separate units as shown in Figure 1, connected by a cable: the Camera Gyro Assembly (CGA), which contains the sensors, and the Data Processing Assembly (DPA) containing the sensor's embedded computer and power supply electronics. The CGA collects raw sensor data upon command and returns the data to the DPA for processing. The CGA provides a simple serial interface to the DPA (or any other flight computer) and directs all necessary timing and control needed by the star camera and MEMS gyros.

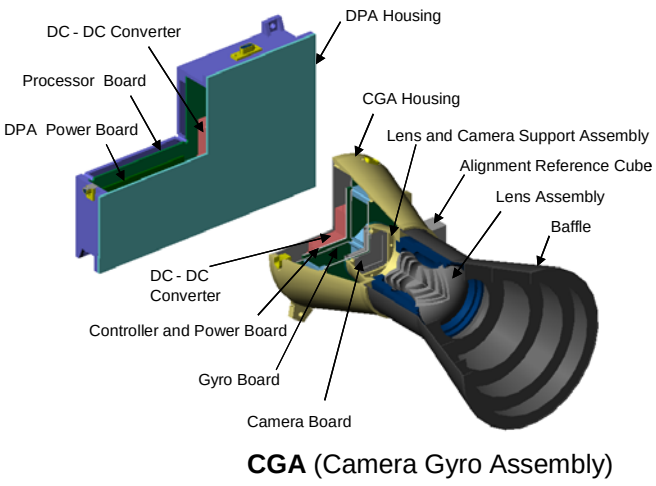

Figure 1 – Component Level Diagram of the ISC

[1] 0-7803-8155-6/04/$17.00 © 2004 IEEE
[2] IEEEAC paper #1358, Version 1, Updated December 09, 2003

The CGA includes the lens, mission specific baffle, focal plane, three MEMS single-axis gyros with analog-to-digital conversion electronics, an interface board, and a 28V, triple output, DC/DC converter. The heart of the star camera is a STAR250 512x512 active pixel sensor array from Fill Factory with an on-chip 10-bit A/D converter. The camera has a command-ready interface to support windowing, various integration times, selectable frame count, and built-in test. The 21º square FOV star camera optics are based on a commercial 35 mm, f/1.2 lens manufactured by Zeiss and modified for space flight applications. Besides the camera subsystem, the CGA houses the gyro subsystem which contains three single-axis MEMS gyros for sensing angular rate. The tiny gyro sensors are etched in silicon using a Draper-developed MEMS process. A sense mass is driven into oscillation by electrostatic motors. The mass oscillates in one axis and as the body is rotated, the Coriolis effect causes the sense mass to oscillate out of plane. This change is measured by capacitive plates and is proportional to the rotational rate of the body. The CGA is 16 cm high (without mission specific baffle), approximately 17 cm wide at its circular base, weighs 1.3 kg and consumes 2 W of power.

The DPA contains an Atmel ERC32 processor, power supply electronics (PSE), and a 28V, single output, DC/DC converter. The DPA interfaces to a host spacecraft via a 3-wire, bi-directional, asynchronous RS422 serial port. Input rates are 9600 baud with a variable output data rate to 38.4K baud. The large downlink capability of the ISC can support transmission of raw imagery from the star camera in addition to the transfer of highly sampled raw and compensated gyro data from the gyro electronics. All of the embedded software necessary for ISC operation runs internal to the DPA. The DPA measures 15 cm x 23 cm x 4 cm, weighs 1.6 kg and consumes 1.5 W of power.

The two-unit design facilitates a simpler integration with a host spacecraft. Only the CGA needs to be precisely aligned with the host spacecraft using the reference cube located on the CGA housing. The modular design was emphasized for operability by allowing concurrent development and testing of the two units. In addition, the modular design suits interesting future applications and variations of the ISC. [1]

A simple system data flow is described in Figure 2. During operation, attitude information is propagated by the ISC's MEMS gyros. The gyros sense inertial rates that are sampled at a high frequency (320 Hz). The raw gyro data is compensated and processed through a Kalman filter to produce the attitude quaternion, which is transmitted to the host spacecraft in real time, at a frequency of 5 Hz. The star camera is used periodically (every few minutes) to obtain a camera quaternion that enables the gyro errors to be removed and the inherent drift of the gyros to be calibrated and compensated. Stars in the image are identified using a lost-in-space (LIS) attitude determination algorithm that analyzes the image against a stored star catalog to help identify the camera's orientation without any prior knowledge of the spacecraft's attitude. [2] Once initialized, the gyros are used to maintain attitude knowledge continuously until the next stellar update can be obtained to support gyro compensation. The complementary use of the gyros and camera data help the spacecraft overcome difficulties in providing attitude knowledge during transients, high slew rates (up to 40º/s), or periods of star camera occlusion. [3]

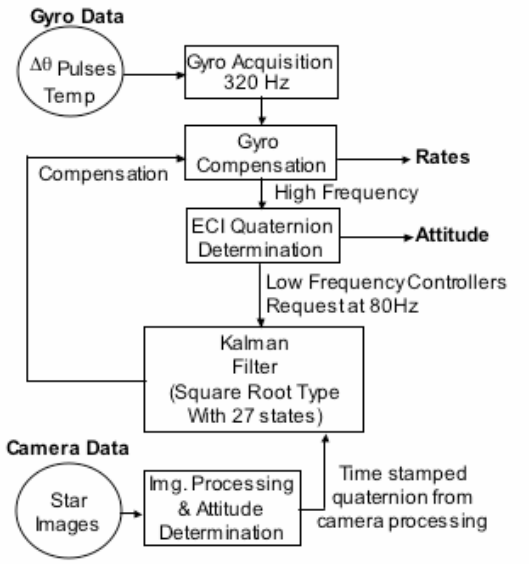

Figure 2 – Overview of ISC Data Flow

2. VALIDATION APPROACH

A rigorous suite of ground and flight tests will accomplish technology validation. Draper will conduct a series of analytical measurements, computer simulations, rate-table tests, star simulation tests, and night sky observatory tests to validate the concept on the ground. These tests will characterize the performance of the ISC over varying camera update rates, angular slew rates, and temperature ranges. The ISC validation objectives are shown in Table 1.

Table 1 – Validation Objectives

Objective	Where Tested	Metric
Accuracy (1-sigma) in each axis with slewing < 40 deg/s	Ground & Flight	0.1 deg
Self-initialization	Ground & Flight	< 10 min over 90% of sky
Power	Ground & Flight	< 4.5 W
Mass	Ground	< 3 kg
Space Qualified Component	Ground & Flight	Operates in typical Earth orbit environment

Flight vs. Ground Allocation

Flight validation of the ISC will demonstrate to potential users that the ISC is a mature, space-qualified technology (Technology Readiness Level 8). Prior to this flight, the ISC is going through an exhaustive ground validation process, intended to maximize the chance of on-orbit success. To the extent possible, the allocation of validation tests is biased toward ground testing for better visibility and control of the system and assurance of test completion.

During flight, specific on-orbit tests will verify, for the first time in a space environment, performance of the MEMS gyros; Angle Random Walk (ARW), scale factor, and bias stability. The ISC's predicted camera performance (dim star limit, chromatic and astronomical aberration, sun and moon keep out angles) will also be validated in the relevant space environment. The integrated performance of the MEMS gyros and APS star imager will be demonstrated under various 3-axis maneuver profiles.

3. GROUND VALIDATION

Overall Roadmap

Having discussed overall ground validation for the ISC program, a more detailed description of the process of ground validation follows. The validation flow was structured along the natural functional lines of the overall system, with subsystems validated separately and the flow gradually building up to validation of the fully integrated ISC system. A top-level overview of the entire process is provided in Figure 3.

The ISC system-level validation encompasses many potentially labor-intensive steps that would traditionally be required in the integration of a suite of separate attitude determination sensors onto a spacecraft. The ISC system validation process shown in the figure is inherently complex because the ISC integrates several sensors. This complexity is a burden shifted from the spacecraft integrators to the instrument designers, to the benefit of both parties. On one hand, the team performing sensor integration with the spacecraft sees reductions in cost, risk and schedule because integration is greatly simplified. On the other hand, the instrument designers, with their detailed knowledge of the internal workings of each sensor, are best prepared to attack the complexity of blending different attitude measurements in an optimal fashion.

CGA Testing

Testing and validation of the CGA was generally focused on the sensors themselves, namely the APS imager and the MEMS gyros, along with their associated electronics. Many test procedures were developed using prototype components. The order of the tests was dictated primarily by hardware availability. As data from each test was matched to analytical models, the team built confidence that the CGA would meet design specifications that could only be measured at the end of the validation process through integrated testing.

CGA Engineering Model—Many test procedures were developed using the CGA engineering model, for later application to the flight CGA equipment. The EM CGA was built around the same board designs as the flight unit, with a

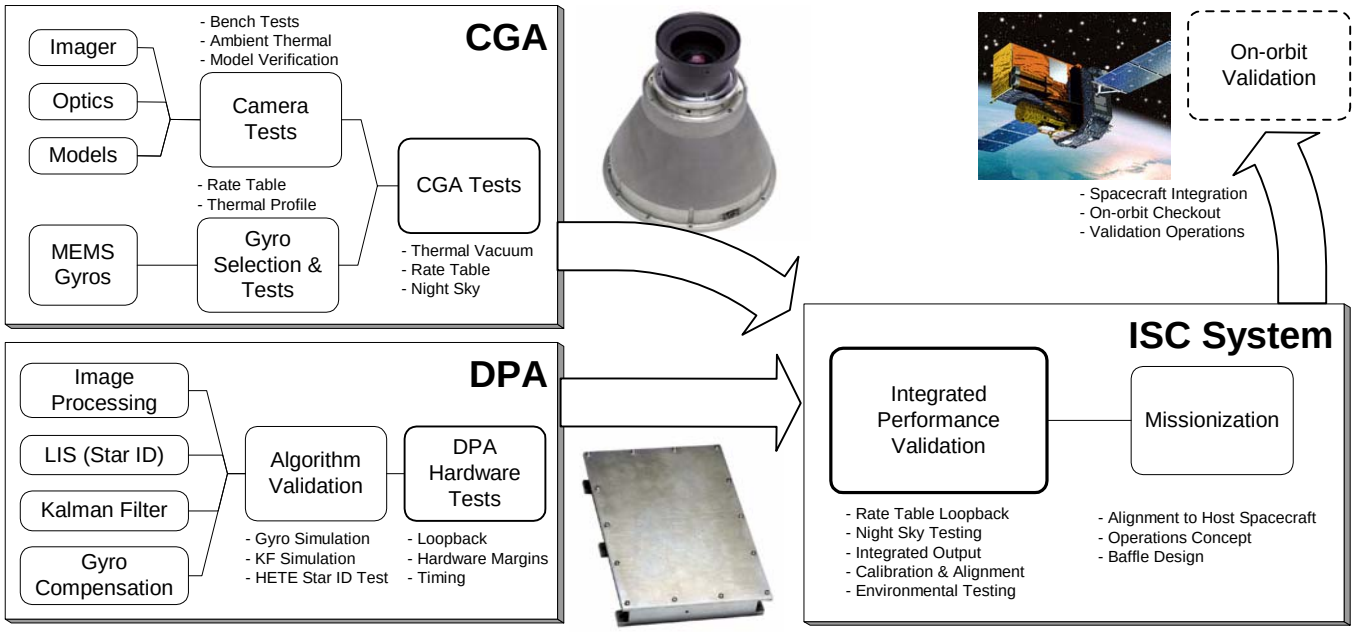

Figure 3 – ISC Ground Validation Process Overview

side-by-side board placement providing easy access. The EM gyro consisted of one single-axis gyro (as opposed to three in the flight unit), and could be swapped with simulated 3-axis gyro inputs from a gyro simulator. The EM camera was fitted with a Canon lens, using a simple adapter mount.

Ground Support Equipment—Testing of the CGA was performed entirely without the DPA. Serial data was acquired directly from the CGA interface, using a Linux PC suitably equipped with a data acquisition card. Software was written in C to command CGA settings and to format the raw serial data from the CGA into engineering telemetry, gyro data files, and FITS (Flexible Image Transport System) images.

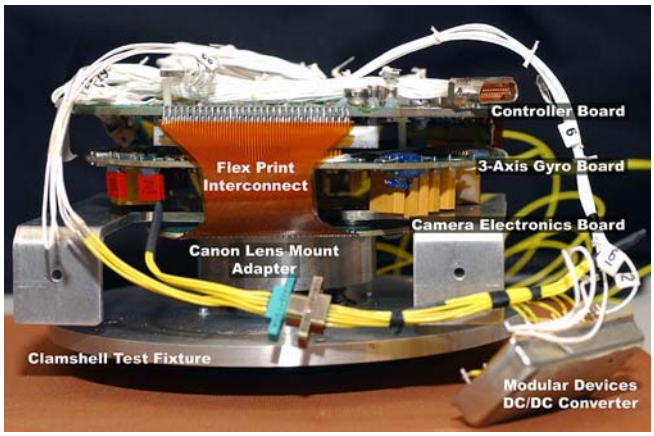

Figure 4 - Flight unit CGA boards on clamshell jig for hardware checkout

APS Camera Testing—Camera tests are described roughly in chronological order. The test campaign broke down into four phases, each using a different test setup. Some preliminary tests were conducted on the bench top with the EM camera. Next, the bulk of camera testing was performed with the flight unit CGA in the thermal vacuum chamber with the star simulator shining in through a window. Following this, some tests were performed on the rate table, again using the star simulator. Finally, night sky tests provided the ideal environment to confirm parameters that were previously measured in the lab.

Camera Analytical Models—Models of increasing levels of fidelity were developed to understand the relationships between key design parameters and their effect on overall performance of the camera. Low-fidelity models were developed very early in the program, to support conceptual design.

Later in the ISC design process, the low-fidelity models evolved into two major high-fidelity Monte Carlo analytical models, created in MATLAB. The pixel-level model was designed to simulate the physical characteristics of the APS chip. The results from this microscopic model (5x5 pixel array) were rolled up into lookup tables used in the field-of-view (FOV) level model, which simulated the performance of the camera on the scale of an entire image frame. The models provided insight into the effect of various operating conditions on the attitude error statistics of the camera, which are ultimately the only numbers that matter in the camera's contribution to overall instrument performance.

The pixel-level model took into account the following sources of error, modeled directly from the specifications of the APS imager: imager noise (fixed pattern noise, dark current, pixel response), interpolation error arising from the centroiding algorithm, and position errors arising from motion of the camera across a star field.

The FOV-level model took into account the results of the pixel-level model and additional error sources that occur across the entire image, including optics-imager alignment shifts (i.e. calibration errors), astronomical aberration, line scan aberration (since the APS is a line-scan device with line-to-line offsets in exposure), and the number of stars and their distribution in the field of view. The model also simulated the process of least squares fitting against the star catalog using the Wahba optimality criterion [4]. Over a large number of runs, the FOV-level model produced error statistics for the entire camera subsystem.

The models allowed an analytical exploration of design tradeoffs and were used notably to pick the final optics configuration (focal length, f-number). They also served to predict camera performance at high temperatures, and expected tracking rate limits. As hardware was built and became available for testing, the results from each test were matched against predicted values computed using the analytical models. Any discrepancies were investigated and on several occasions uncovered minor errors in the models.

Camera Solar Exposure—The aperture of the ISC lens is necessarily larger than for a typical star tracker because the ISC is a wide field of view instrument using an APS sensor. Therefore, there was concern that prolonged exposure to the sun while the camera was operating might damage the imager. A realistic solar exposure test is difficult to perform without a solar simulator shining into a vacuum chamber, so a simpler, limited test was performed. The EM camera was taken outdoors and exposed to the June sun on a very clear day, under ambient pressure conditions. To detect any damage to the imager, dark frame and sensitivity tests were performed before and after exposure. The imager passed this test without any discernable effect, but it is unknown how much design margin exists with respect to the space environment, where atmospheric attenuation and air convection are both absent and increase the amount of heat absorbed by the imager.

Camera APS Chip Selection—Three STAR250 Active Pixel Sensor chips were available for use in the flight unit. All three were placed in the EM camera board and underwent a

temperature sweep over the entire thermal operating range. Dark frames were acquired throughout the test, and manually analyzed both for temperature behavior and the amount and distribution of bad pixels. Then, each chip was tested for sensitivity using the EM optics and star simulator, at a setting of Mv ~ 2.5. Interestingly, the three nominally identical chips showed measurably different characteristics under identical test conditions. One chip was eliminated for its higher sensitivity to temperature variations, and another was eliminated because of two adjacent defective pixels that could trick the image processing algorithms into detecting a non-star "spike". While the star identification algorithms handle spikes easily, the sensor with the fewest cosmetic defects was chosen.

Camera Ambient Pressure Focus—With the flight camera assembly complete, preliminary focus was established iteratively by using a set of plastic lens shims. Focus was measured via spot size, by fitting a two-dimensional Gaussian to images that were produced using the star simulator. Perl and MATLAB image processing scripts automated this process so large numbers of star images could be quickly analyzed. Once preliminary focus was established, a set of metal shims was fabricated to cover a narrow range of focus settings overlapping the known vacuum focus shift of the optics, which had not been measured. Not surprisingly, repeatability of the focus measurement was much better with a single metal shim than with a stack of soft plastic shims. The focus test also provided a measurement of the smallest spot size achievable with the optics.

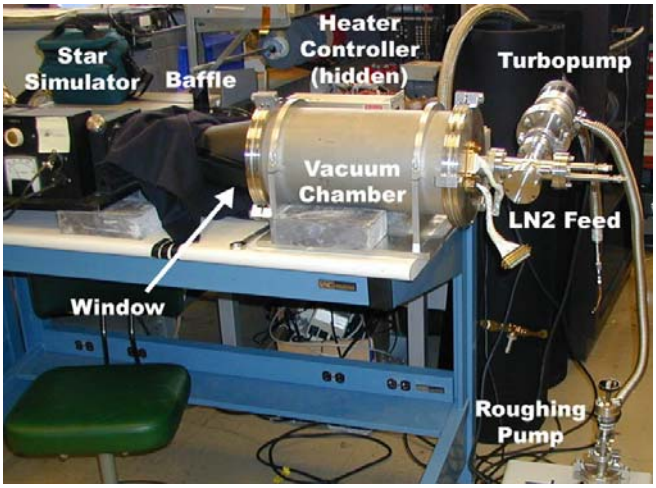

Figure 5 – Thermal Vacuum setup, MIT Center for Space Research.

Camera Noise Equivalent Angle (NEA)—The single-star NEA performance was measured in the TV chamber, using the star simulator, and compared to the camera analytical models. The test was performed in the middle and at the top of the imager's operating temperature range. Large sets of consecutive star images were analyzed using the image processing algorithms to extract centroid locations. The NEA displacement statistics were computed from the centroid data using a MATLAB script. NEA testing was hamstrung by the poor calibration and stability of the star simulator at higher magnitudes, since much of the interesting behavior of NEA occurs near the sensitivity limit of the imager. This measurement will be repeated during an upcoming night sky test.

Camera Chromatic Aberration—The chromatic aberration test was performed with the star simulator and TV chamber setup. Kodak Wratten color filters were placed in front of the chamber window, and changes in star image spot size and location were monitored. Unfortunately, the poor optical quality of the filters badly degraded the star images causing reliance on the chromatic aberration figures provided by the lens manufacturer. This was deemed an acceptable approach because the lens was a widely produced design and chromatic aberration was not a dominant source of error.

Camera Vacuum Focus—The vacuum focus was measured using the same method as in the ambient pressure focus test, but this time in the TV chamber with the star simulator shining through the chamber window. Since focus was measured indirectly through spot size, it was necessary to first measure the effect of the TV chamber window on spot size. Three different measurements of spot size were made: first, without the chamber window, second, with the window at ambient pressure, and third, under vacuum. The results showed that the chamber window has a negligible effect, and that the focal length shortened exactly as expected. Once vacuum focus was set properly with the desired shim thickness, a few other focus tests were performed. Off-axis focus was tested in several places near the edge of the image, to verify that there was no variation in spot size across the image. De-mating and re-mating the lens to the CGA provided a test of focus repeatability. Finally, the temperature of the TV chamber was varied to verify that focus was constant over temperature, using a temperature range slightly wider than the nominal operating range.

CGA Thermal Vacuum—The thermal response of the CGA hardware was tested in the TV chamber over a variety of temperature ranges, operating or not, in order to obtain sufficient data to validate the analytic thermal model of the instrument. The temperature was controlled at the base plate of the instrument, and the chamber walls remained at ambient temperature. The CGA was wrapped in several layers of Mylar to minimize radiative coupling of the CGA housing to the chamber walls. Calibrated thermocouples were placed in two locations, and an additional four temperature points were provided by the CGA electronics (imager temperature and gyro ASIC termperatures.) Overnight temperature soaks were performed over the entire operating range of the CGA.

CGA Thermal Survival—Using the same thermal vacuum setup, the un-powered CGA was exposed to temperature extremes under vacuum. Following several hours of exposure, the CGA temperature was brought back into its operational range, and a functional test was performed to confirm survival.

Camera Dark Frame—The approach used to compensate raw images for dark current effects was constrained by DPA memory, which could only store a single dark frame. A dark frame compensation method was devised to scale this single "master" dark frame to any desired temperature, using a temperature lookup table. Dark frames were collected during thermal vacuum testing over the entire operating range of the camera. At several temperature points over the operating range, a large number of dark images were collected and averaged together to produce a mean dark frame at each particular temperature. The averaging process removed background noise and yielded the average background level for each mean dark frame, as a function of temperature. The average background level over temperature was compiled into a simple lookup table. The master dark frame, to be stored in DPA memory, was picked out from the collection of mean dark frames, near the upper end of the temperature range where dark current effects are the most significant. The dark frame scaling method is not exact because individual pixels have slightly different dark current behavior as a function of temperature. The extent of residuals induced by the method was measured by comparing the master dark frame scaled to a particular temperature with a mean dark frame acquired at that temperature. This test showed that a concern would only exist at the highest temperatures, and could be addressed by tuning the star detection thresholds of the image processing algorithm.

Camera Rate Tracking—This test verified performance of the camera against the tracking limit specification of 0.25 deg/s. The test was performed with a single moving star, with results matched against the analytical models. The CGA was mounted on a rate table with the rotation axis of the table parallel to the boresight. The star simulator was set up a few degrees off-axis such that a star would describe a circle on the image plane when the table was rotated. Images were acquired as the table was spun at different rates. The blurring effect of camera motion is worst when the boresight is perpendicular to the axis of rotation. Since the test setup did not simulate this condition, the rate table had to be driven at a higher compensated rate to account for the smaller angular separation between the spin axis and the simulated star. At each table rotation rate, a series of consecutive images was collected. Any two consecutive images of the same star should in theory have shown exactly the same relative spacing, because the timing of the camera electronics ensured that successive images were collected at rigorously uniform intervals. In practice, the smearing of the image degraded the performance of the centroiding algorithm and introduced errors in the measured position of the star. By measuring the variability in the spacing between two consecutive images of the same star, the "jitter" or position error that arose from the motion was extracted and compared to the analytical models.

As the rotation rate was increased, the star position error was not the only factor that influenced tracking performance. The motion smeared out dim stars and caused them to become undetectable, an effect that eventually decimates a star field to the point that too few stars are picked up for star identification. This aspect of the problem was not investigated in this test because the calibration of the star simulator was suspect in the relevant magnitude range. Ultimately, a comprehensive test of tracking performance will be conducted in further night sky tests.

Camera Calibration Parameters—The camera calibration consists of five parameters: focal length, two components of the optical center, and two radial lens distortion coefficients. These five parameters are used to translate the pixel coordinates of a star image into a body-fixed unit vector in the direction of the observed star. The quality of the calibration affects not only the accuracy of the final computed attitude, but more importantly the performance of the star identification algorithm.

For the optical center measurement, the initial approach was to use the batch method of Samaan et al. [5] on a large sample of night sky images. However, trials with this method showed that the optical center was poorly observable, with converged estimates varying by large amounts between different images. Another method was devised somewhat accidentally, when it was noticed during the rate tracking test that the lens filter produced a strong ghost image when the star simulator was set brighter than Mv = 0. Intuitively, the ghost image would appear exactly opposite the optical center from the primary image, assuming the filter plane was exactly normal to the optical axis. To relax this latter assumption, the CGA was rotated about the boresight and ghost images were acquired over one full revolution, in order to eliminate the effect of filter misalignment. At this point, the optical center was measurable down to the mechanical tolerance between the optical axis and the rate table axis, which was significantly better than the variability observed in the night sky method. Using MATLAB scripts, the resulting images were reduced and averaged to produce the two calibration parameters of the optical center.

With the optical center known, the focal length was measured using the batch method of Samaan et al. A sample of twenty images from different parts of the sky acquired during various night sky sessions was used to compute the focal length. The most time consuming aspect of this process was star identification, which had to be performed by visual comparison of each image to stars in the Hipparcos catalog. The batch method was then applied to each image, and residuals were monitored to ensure that no

errors were made in star identification. The final focal length calibration parameter was calculated by averaging focal length measurements extracted from each image, weighted by the number of stars in each image. The result was then compensated for the known vacuum focus shift, since the night sky images used for the calibration were not acquired under vacuum.

The two radial distortion calibration parameters are the coefficients of an even, fourth order polynomial function of the distance of a star from the image center. They were extracted from the same images used for the focal length calibration. For each star in the data set, two parameters were calculated: the measured angle from boresight, and the true angle from boresight. (to obtain the latter, the "true" J2000 boresight vector was calculated by performing a least squares fit on each image.) Once the radial position error for each star was known, a fourth-order polynomial fit was applied to the entire data set, with the constraints $f(0) = 0$ and zero odd coefficients. For this wide field of view optical system, the radial distortion calibration turned out to be critical, notwithstanding the high quality of the optics.

Camera Sensitivity—An accurate measurement of imager sensitivity was not obtained until the CGA was exposed to the night sky, where star magnitudes are well known. Had the star simulator available for lab testing been better calibrated and more stable, an earlier measurement would have been possible. The first night sky test using the flight CGA unit provided proof that the sensitivity matched the predictions of the analytical models. The temperature dependence of sensitivity was also tested, by heating the CGA base plate with a hair dryer and monitoring performance as a function of imager temperature.

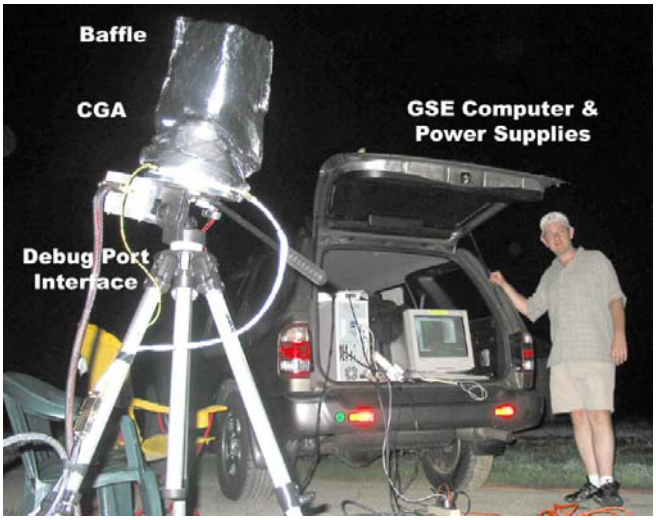

Figure 6 – Typical CGA-only night sky test setup at MIT Wallace Observatory in Westford, MA. The CGA is bagged for protection from condensation and insects.

MEMS Gyro Testing—The ISC leveraged an existing gyro design, repackaged with radiation hardened, de-rated parts. To mitigate risk, a single axis gyro assembly was built to verify that ARW (Angle Random Walk), scale factor and bias stability met ISC system specifications. Subsequently, the three-axis flight board was built. The gyros and ASICs were subject to thermal cycling and a random vibration test. Concurrently, each set of support electronics was installed and tested over temperature on the gyro board. The gyros and ASICs were then installed on the board, and a resistor for each axis was selected to set the maximum dynamic range. For the ISC application, it is set to a little over 40 deg/s. Each axis was rate tested under a ramped thermal profile. Then the complete three-axis gyro board was assembled in a test fixture and mounted on a two-axis rate table with thermal control. The three-axis gyro board was run for several thermal cycles over the entire CGA temperature range while subjected to various rates. The bias and scale factor temperature sensitivities were derived from these test results. In addition, long term ARW and in-run bias data was also collected. This incremental build and thermal test approach has proven to be the most efficient method and produced a 3-axis MEMS gyro board meeting all specifications with the first build.

DPA Testing

Thorough hardware and software tests of the DPA (see Figure 3) were required before integrated tests with the CGA. This included testing of the processor board, PSE (Power Supply Electonics), a DC/DC converter, and the embedded flight software.

Processor Testing—Hardware testing was conducted for the functions listed below. Most notable was running the ERC-32 at 4MHz, which is much lower than its capability. This allowed for significant power reduction and yet easily met the ISC throughput requirements.

- ERC-32 clock speed reduced to 4 MHz
- Power-on reset
- Built-In Test (BIT) function
- EDAC protection on SRAM and DRAM
- Watch dog timer timeout period and disable
- System clock set and adjust
- Interface to a host, CGA, GSE test computer
- Gyro data from the CGA at 320 Hz
- 3.3 V and 2.5 V power control
- Gyro packet time tagging
- Camera data acquisition at 1 Megapixel per second
- Camera frame time tagging

Algorithm Testing—Traditionally, attitude determination algorithms are separately developed, integrated and tested by the spacecraft developers integrating the sensor suite. As an integrated attitude sensor, the ISC will significantly unburden these spacecraft developers by having all the algorithms pre-integrated and tested within the instrument. The four major ISC algorithms relate to image processing, star identification or Lost-in-Space (LIS), gyro

compensation and Kalman filtering. The algorithm relationships and data flow are shown in Figure 2.

Image processing algorithms were developed early in the program using an evaluation camera that contained the STAR250 imager. This allowed the camera design some degree of simplification and risk reduction since actual camera output was being used for testing the algorithms.

The LIS algorithm was developed and tested prior to inclusion with the ISC. Daniele Mortari and his associates developed, tested in simulation, and published their results on this very robust algorithm [2, 7]. When the algorithm was selected for inclusion in the ISC, it was tested with images produced by the ISC evaluation camera during a series of early night sky tests. The algorithm was tested with both a software simulation and the DPA hardware to ensure correct porting of the software. In addition, the algorithm was flight verified on the HETE-2 spacecraft [6], which ultimately gave the program significant confidence in its reliability and robustness.

The gyro compensation equations were verified in a MATLAB simulation. The coefficients typical of the flight system were applied to the equations. The ISC software receives raw gyro data at 320 Hz and reduces it to 80 Hz with a median filter prior to processing by the Kalman filter. Deterministic 320 Hz raw gyro and temperature data was provided to the simulation in order to verify expected compensated output. In addition, various data with spikes or off-nominal points were also supplied to verify the robustness of the compensated output.

The twenty-seven state Kalman filter was written in C and tested in a standalone C simulation. The filter provides gyro-based attitude estimate, error estimate, and continuously updates gains for each state. ISC Kalman filter states are:

- 3 for attitude error
- 3 for turn on bias (deg/hr)
- 3 for turn on scale factor (ppm)
- 3 for Markov bias stability over time (deg/hr)
- 3 for bias stability over temperature (deg/hr)
- 3 for Markov scale factor stability over time (ppm)
- 3 for scale factor stability over temperature (ppm)
- 6 for alignment (each axis has 2 DOF alignment)

The Kalman filter was configured as a drop-in module that could be used interchangeably with the simulation or the embedded flight software. This simplified debugging, freed up hardware resources, and allowed filter tuning to proceed in parallel with other tests. Simulation runs were performed with a wide range of inputs including deterministic gyro data, camera quaternion updates and various sources of error. The filter was tuned based on Monte Carlo runs that determined to which input parameters and errors the Kalman filter was most sensitive.

Each of the algorithms were then hosted on the ERC-32 simulator package with RTEMS (Real-Time Operating System for Multiprocessor Systems). Timing, throughput and memory allocations were verified prior to installing and testing on the flight hardware. This step proved to be critical because most of the remaining bugs found during integrated tests were confined to the transfer and storage of CGA data.

Integrated Testing

Integrated testing includes bench testing, rate table testing and night sky testing.

Bench Testing—This critical portion of the test program allowed us to develop the necessary GSE and software ground tools to provide visibility into the inner workings of the ISC. Bench testing was first performed on the breadboard system, and later on the flight system prior to packaging into the housing.

All commands and telemetry going between the ground station computer and the DPA were formatted in CCSDS (Consultative Committee for Space Data Systems) packets. This interface was tested using a batch scripting capability that exercised each command and verified the expected response. Scripting made testing fast, easy and repeatable.

The camera was designed with five test patterns that could be commanded from the ground: incrementing columns or rows, alternating columns or rows and a single user-defined threshold. This allowed us to verify that every pixel was being sent from the CGA to the DPA and on to the ground station without any corruption.

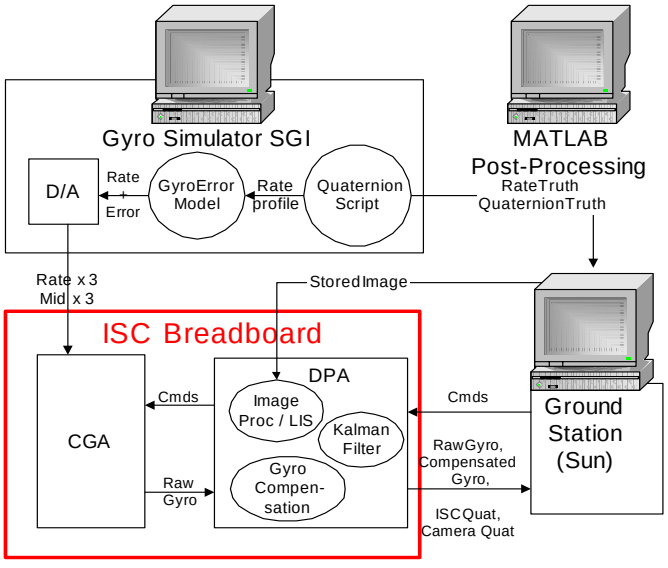

Figure 7 - Gyro Simulator Setup

Sky images can be uploaded from the ground station computer to the DPA to test image processing and LIS algorithms. Using images acquired in early night sky tests from the evaluation camera or the CGA by itself, the upload capability allowed algorithm testing to proceed well before night sky testing of the integrated system, giving some assurance that the ISC would self-initialize. Conversely, the raw image being processed can be downloaded to the ground station to aid in debugging.

The gyro simulator GSE was critical to early debugging of the flight software. This allowed any simulated rate profile with gyro error sources to be applied directly to the A/D inputs on the gyro board as shown in Figure 7. Sine waves applied at various frequencies and amplitudes were quite effective in assuring that the flight software was receiving the expected signal with the correct signs, magnitude scaling, time sequential order and from the correct source.

A loopback mode was created to facilitate Kalman filter testing within the lab. When operating in loopback mode, the ISC processes a series of stored images in conjunction with gyro data from the flight gyros or from the gyro simulator. This mode was the single most important mode for testing the breadboard or flight system in a lab setting. It exercised all the functionality and flight software with the exception of the optics and the APS imager. Using the gyro simulator, batch testing was performed over various rate profiles, with error parameters doubled or even tripled over specification to verify system response.

Rate Testing—Unlike many other attitude systems, the three-axis rate output of ISC is pre-compensated over temperature for bias, scale factor and axis misalignment. A two-axis rate table with thermal control (Carco Model 57CD) allowed each gyro to be accurately characterized over a range of rates and temperatures. The scale factor, bias, and axis misalignment errors were accurately measured by comparing the ISC rate data output to the rate table truth data. From these errors a set of gyro compensation coefficients were calculated and uploaded to the ISC software. The ISC was then rerun over the same range of rates and temperatures to verify the compensated output had errors reduced to below specified levels.

The two-axis rate table was also used to verify the integrated output with the flight hardware configured as shown in Figure 8. The ISC was commanded into loopback mode to performed LIS on a stored image and receive inputs from the flight gyros. Rate table motion was imparted between camera updates, always returning to the same orientation for each update. This allowed the ISC accuracy and power consumption to be verified over temperature, with different camera update intervals, and various rate and total angle profiles. It was not possible to fully compensate for Earth rate using the two-axis rate table, so this was left as a bias for the ISC to filter out. A planned three-axis rate table test will allow not only Earth rate compensation, but also more complex attitude profiles with image updates at different attitudes corresponding to multiple stored images. In the meantime, to make up for this limitation, the multiple image cases were verified using the gyro simulator instead of rate table inputs.

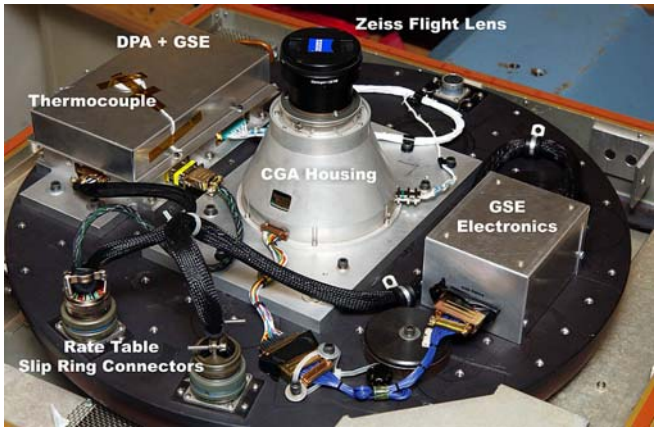

Figure 8 - Rate table setup with thermal cover removed.

Night Sky Testing—Testing performed under the night sky, with the fully integrated ISC, went considerably beyond the CGA-only night sky tests described under camera testing. The purpose of integrated night sky testing was to prove that the sensors and algorithms worked together and produced the required attitude determination performance under a variety of operating conditions. While the Boston area provided only rare nights with optimal weather and lunar conditions, night sky testing provided the highest fidelity environment in which to test the ISC.

One of the most important checks performed in the lab prior to night sky testing was an end-to-end verification of the polarity of sensor outputs through the many steps involved in obtaining ISC outputs. Sensor data was examined at each step along the way, including raw measurement in the CGA, serial data transfer to the DPA, storage and processing in the DPA, CCSDS telemetry data transfer to the ground station computer, and finally telemetry display routines. With the CGA mounted on a tripod, motion was imparted manually about each axis to verify the polarity of gyro telemetry. A test pattern was placed on a wall and imaged with the camera, verifying that pixel coordinates were being handled correctly.

The first set of integrated night sky tests was performed by mounting the DPA and CGA on a simple photography tripod. Two computers were used to acquire data from the system, a Sun workstation communicating with the DPA, and a Linux PC monitoring the outputs of the CGA via its debug port. Being able to monitor the CGA outputs proved invaluable to the process of tracking down bugs in various parts of the flight software, especially in the area of data transfer and storage. While it was never expected that the system would produce a valid quaternion under its first night-sky exposure, a valid quaternion was produced after

the lens cap was removed for the first time. This was accomplished despite poor observing conditions, the lack of camera calibration and several then-undiscovered software bugs. The instrument was manually moved over various portions of the sky to excite the gyros. Finally, the ISC was pointed to zenith for over an hour to collect attitude data with earth rate as the only motion. The tests gave the first operational look at Kalman filter performance and camera accuracy.

The second set of integrated night sky tests placed the ISC on a tracking telescope mount, stabilized on a concrete pier, with independent real-time readout of Right Ascension (RA) and declination (DEC). The night sky setup is shown in Figure 9.

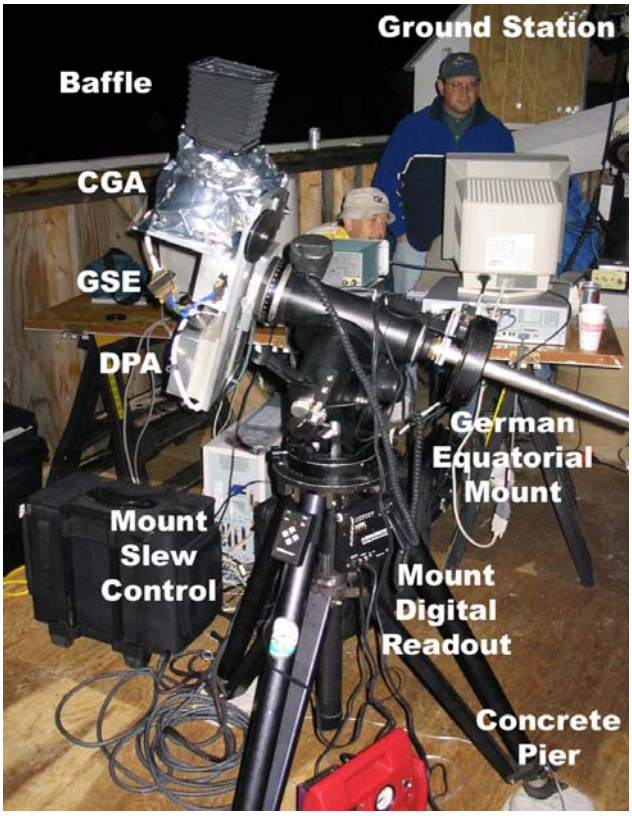

Figure 9 - Integrated Night Sky Setup at the Amateur Telescope Makers of Boston facility in Westford, MA.

The mount readout was calibrated directly using the ISC by sighting in the direction of bright stars and monitoring the ISC output quaternion, suitably converted to RA and DEC in the telemetry decoding software. As the mount was steered to different portions of the night sky, it provided a reference "truth" attitude profile that could then be matched against the integrated quaternion output of the ISC. A sample run is shown in Figure 10, showing RA as a function of time. The red line represents the integrated ISC output, and is plotted against the black line representing the RA output of the mount. Note that before the 350 second mark in the figure, the ISC has not yet finished initializing, so its output has not fully converged to the truth data.

The mount provided the ability to slew the ISC in a controlled fashion, a marked improvement over the coarse motions imparted during previous tests using the photography tripod. The different tests produced extensive data sets for further Kalman filter tuning and demonstrated that the camera met its performance specifications over a significant portion of its operating envelope.

A more comprehensive night sky test is planned specifically to probe the edges of the operating envelope. The CGA will be placed inside a thermal enclosure and driven to its temperature extremes while operating in order to characterize its degradation in performance as temperature limits are exceeded. Further tests will also be performed, including rate tracking to quantify the rate limit on a real star field, high-temperature NEA measured on dim stars, and final tuning of the Kalman filter.

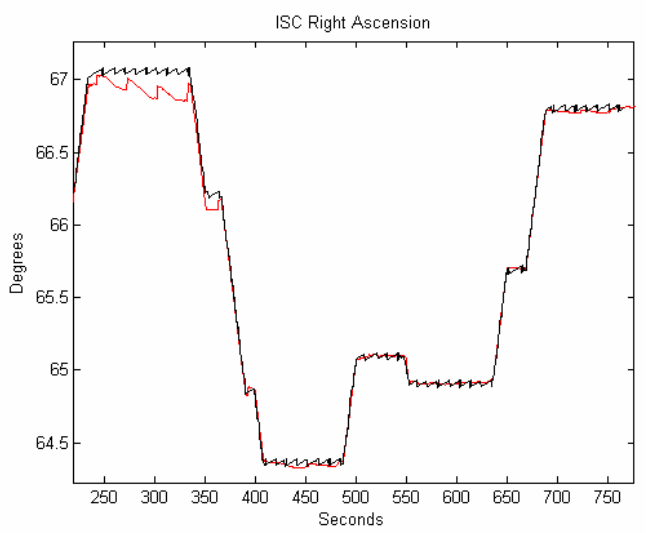

Figure 10 – Sample output of night sky testing, showing Right Ascension vs. time with occasional slewing motion applied to the ISC.

Environmental Testing

For space qualification, the ISC will be subjected to a full complement of environmental tests. This includes ten cycles of GEVS-specified (General Environmental Verification Specification) thermal vacuum tests for both the DPA and CGA. During thermal vacuum testing only, a star simulator will be used to exercise the camera through a window in the chamber. For vibration testing, a low-level sine vibration sweep of each axis will be conducted to verify predicted resonances. Random vibration and shock tests will be conducted in each axis to proto-flight levels for Ariane 5. While the ISC is designed to be immune to spacecraft level EMI interference, a full quota of MIL-STD-461 EMI/EMC tests will be conducted, in addition to EMC compatibility testing on the host spacecraft.

4. LESSONS LEARNED

Lessons learned (so far) are provided in the hope that they might be of value to similar sensor technology programs. Since they cover a wide range of topics, they are provided in no particular order.

Things That Were Good

Loopback Mode—The loopback test capability proved to be very effective and uncovered many of the bugs with the software and the Kalman filter. This mode will allow for the highest fidelity of ISC operation during spacecraft integration and test.

Gyro Simulator—To reduce the reliance on rate table testing and to complement loopback mode, the gyro simulator was used to apply simulated motion profiles to the breadboard hardware. These profiles were injected in analog form and digitized within the breadboard CGA, exactly as the analog data from the MEMS gyros. The gyro simulator provided the capability to apply any desired simulated motion profile, with or without error sources, in a controlled and repeatable fashion.

CGA-DPA Data Link Monitoring—The CGA was designed with a "sniff" capability to independently monitor the CGA-DPA serial data link through the CGA debug port. This port interfaced via a non-intrusive optical coupling to existing CGA GSE (see lesson learned: Early GSE Development) and acquired image frames, gyro data, and housekeeping information in order to gain insight into the operation of the CGA, even while it was under DPA control.

Early GSE Development—GSE built to act as an effective DPA simulator was crucial to the early design and prototype of the CGA breadboard hardware and image processing algorithms. Hardware was designed to replicate the agreed-upon controlled interface to the CGA, which enabled rapid prototyping of software in a Linux environment. The same GSE later allowed checking the CGA's functionality independently from DPA operations.

Camera Modeling—To avoid the common pitfall of "analysis paralysis", both low and high fidelity camera models were developed at different times in the program. The low fidelity models got the design started quickly and the later-developed high fidelity models allowed the design to progress with confidence.

Night Sky Testing—There is no substitute for night sky testing, even when all the other ground testing has been completed to a high degree of satisfaction. The night sky tests verified expected sensitivities, accuracies, and operating modes of the ISC. Achieving a night sky test in New England can be challenging due to weather, high dew points, hungry insects, and a fair amount of light pollution but remains nonetheless crucial to ground validation.

Independent Expertise—Independent experts provided a fresh perspective on many design challenges encountered along the way. External reviewers routinely provided insight into necessary and sufficient testing procedure to accommodate validation.

Community Involvement—The program collaborated with the Amateur Telescope Makers of Boston during the night sky testing phase. This community group generously provided time, expertise, equipment, and an observing facility suitable for ISC testing.

Program Momentum— The motto – "fine it does not work for now, move on" helped to maintain forward progress on the program. Problems were exposed, categorized, and prioritized by groups. Often, an underlying root cause would reveal itself and be fixed, usually solving more than one problem.

Using Standards—A concerted effort to use standards whenever possible avoided custom software design and simplified interconnectivity. CCSDS was implemented in telemetry along with adoption of the FITS standard for images. An RS422 serial port made for a simple host connection.

Configurable Telemetry Stream—The high data rate, configurable CCSDS telemetry output of the DPA enabled excellent visibility into the system. Multiple commutation "windows" were configured within the ground station computer and the DPA to allow engineers to monitor desired internal states.

Early Development of Image Processing—STAR250 image processing algorithms were developed very early in the program and refined through repeated use, as early as the first night sky test using the evaluation camera. When the flight software was developed, the algorithm needed only porting and no further debugging.

Things That Could Have Been Better

CGA Simulator—To test the CGA fully, a suite of GSE that functionally emulated the DPA was used throughout the program. The converse was not true; a CGA simulator was not built. This caused full DPA testing to be delayed until the CGA was ready, and when it was, the hardware was often needed for other tests.

Two-Axis Rate Table—The two-axis rate table limited our ability to perform loopback testing with multiple images, forcing us to wait until integrated night sky testing to test successive camera updates with varying amounts of slewing between updates. A three-axis rate table facility is currently being configured to support further mission profile verification.

Star Simulator—Using a vintage star simulator with inadequate performance at higher star magnitudes constrained us to rely greatly on night sky testing. A modern star simulator, accurately calibrated, would have allowed us to do more testing in a controlled environment earlier in the program.

Image Upload to CGA—A useful feature for system testing would be the ability to artificially place an image into the CGA in near real time. This capability would allow for the system to be completely checked out on a rate table using images from night sky testing. Currently, images can be loaded into the DPA, but the slow upload speed precludes real time capability and requires loopback mode to be used for system testing, rather than just self-test.

Slow Software Loads—Complex embedded software will always require a large number of revisions. Faster software loads would have enhanced our ability to perform rapid design iterations. Rapid iterations enable faster debugging of embedded software and associated hardware via diagnostic routines.

5. CONCLUSIONS

The ground validation process for the ISC was specifically tailored to the integrated design of the instrument. Bringing together two advanced, complementary sensor technologies such as MEMS gyros and APS imagers required not only individual sensor testing but also substantial system-level testing to ensure the robustness of the instrument over a wide range of operating conditions.

Experience from the ground validation of the first ISC flight unit will establish the necessary framework to develop the integration and test process for future production of this class of instrument. The pre-integrated nature of the instrument considerably simplifies integration with a spacecraft, providing a "bolt-on" attitude determination capability. The spacecraft integration is reduced to mechanical alignment and an Attitude Determination & Control System (ADCS) software interface consisting of the Earth Centered Inertial (ECI J2000) attitude quaternion and attitude rates.

Flight testing of the ISC will space qualify the instrument and demonstrate its capability in the relevant environment. The New Millennium Program is providing the path to validate advanced technologies that have not flown in space, such as the ISC. This will reduce the risk and cost associated with selecting the ISC for future space missions, providing them with the full benefits of this new sensor technology. For an attitude sensor, the ISC's integrated functionality and high-rate capability are unique and represent a step forward in spacecraft technology.

The ground validation of the ISC was conducted in an orderly and thorough fashion to significantly raise its Technology Readiness Level in preparation for space validation.

REFERENCES

[1] T. Brady et al., "The Inertial Stellar Compass: A Multifunction, Low Power, Attitude Determination Technology Breakthrough", *26th Annual AAS Guidance and Control Conference, Breckenridge*, CO, 5-9 February 2003.

[2] D. Mortari, J. Junkins, and M. Samaan, "Lost-in-Space Pyramid Algorithm for Robust Star Pattern Recognition," *24th annual AAS Guidance and Control Conference, Breckenridge*, CO, 31 January - 4 February 2001.

[3] T. Brady et al. "The Inertial Stellar Compass: A New Direction in Spacecraft Attitude Determination", *16th Annual AIAA/USU Conference on Small Satellites*, Logan, Utah, 12 – 15 August 2002.

[4] G. Wahba, "A Least-Squares Estimate of Spacecraft Attitude," *SIAM Review*, Vol. 7, No. 3, p. 409, 1965.

[5] M. Samaan et al., "Autonomous On-Orbit Calibration of Star Trackers", *2001 Core Technologies for Space Systems Conference Proceedings*, November 28-30, 2001.

[6] G. Crew, R. Vanderspek, J. Doty, "HETE Experience with the Pyramid Algorithm", MIT Center for Space Research, Cambridge, MA, 02139 USA. 2003.

[7] D. Mortari, "ESOQ: A Closed-Form Solution to the Wahba Problem", AAS-96-173, *Sixth Annual AIAA/AAS Space Flight Mechanics Meeting*, 11-15 February 1996.

ACKNOWLEDGEMENTS

The authors would like to acknowledge the entire ISC team at Draper, consisting of S. Ashkouri, P. Battstone, R. Brown, J. Campbell, J. Connelly, J. Donis, R. Esteves, R. Haley, T. Hamilton, M. Hansberry, E. Hildebrant, A. Jimenez, F. Kasparian, B. Kelley, A. Kourepenis, D. Landis, M. Matranga, K. McColl, J. McKenna, R. Menyhert, D. Monopoli, R. Phillips, E. Powers, D. Schwartz, P. Sienkewicz, S. Tavan, T. Thorvaldsen, W. Wyman, and J. Zinchuk. The ISC team also acknowledges Roland Vanderspek (MIT Center for Space Research), Daniele Mortari (Texas A&M University), Christian Bruccoleri (University of Rome), GSFC, and JPL for their outstanding contributions to the development of the ISC. A special thanks goes to Bruce Berger and the Amateur Telescope Makers of Boston.

The NASA research described here is being carried out at Draper Laboratory under a contract with the Jet Propulsion Laboratory, California Institute of Technology.

BIOGRAPHIES

Tye Brady *is a Senior Member of the Technical Staff in the systems design and analysis group at Draper Laboratory. He has worked over the past 15 years on spacecraft instrumentation, design, and integration. Before joining Draper, he has worked on numerous satellites including ASCA, HETE, Chandra, Astro-E, and HETE-II as technical research staff at MIT's Center for Space Research CCD Laboratory. In addition, he has served as an expert consultant for the small satellite community specializing in spacecraft hardware systems and the development of low-cost remote ground stations around the world. He holds a BS in Aerospace Engineering from Boston University and a SM in Aeronautics and Astronautics from MIT.*

Sean Buckley *is the leader of the GPS/INS and Avionics Integration group at Draper Laboratory. He has worked over the past 18 years on real time hardware in the loop simulations, avionics integration and environmental test. He has worked on numerous space programs including the Kistler RLV, SPIDR, ARES, several MEMS IMU programs, and tactical programs including the A-10 GPS/IDM upgrade and AH-1W fire control system. He holds a BS and MS in Electrical Engineering from Northeastern University.*

Clem Tillier *is a Senior Member of the Technical Staff at Draper Laboratory. He was system engineer for the OPAL satellite, launched in 2000, and has worked on spacecraft attitude control and constellation maintenance problems. Since joining the laboratory's modeling and simulation group in 2001, his work has included analysis and testing for the ISC camera, conceptual spacecraft designs, distributed simulation using the High Level Architecture (HLA), and other simulation infrastructure projects. He received a BA in Physics from Princeton University in 1994, and MS and Engineer's Degrees in Aeronautics and Astronautics from Stanford University in 1996 and 1998.*